VOL. 15, NO. 21, NOVEMBER 2020 ISSN 1819-6608
ARPN Journal of Engineering and Applied Sciences

www.arpnjournals.com

ANALYTICAL MODEL FOR THE ABSOLUTE SPECTRAL RESPONSIVITY BASED ON SILICON TRAP DETECTORS

Alaaeldin Abdelmageed[1], Moamen R. A. El Sayed[1,2] and Arafa Hassen[2]
[1]National Institute of Standards, Photometry and Radiometry Division, Giza, Egypt
[2]Department of Physics, Faculty of Science, Fayoum University, Fayoum, Egypt
E-Mail: alaa_nis@yahoo.com

ABSTRACT

Responsivity scale for most photometric and radiometric detectors can currently be established with the highest accuracy by using detector-based methods. This achievement in detector responsivity has been largely stimulated by the availability of high-performance, low-cost, solid-state detectors like silicon trap detectors. This work aims to develop an analytical model for responsivity scale based on silicon trap detectors over the wavelength range from 300 nm to 1000 nm. This model is considered as a modified ideal quantum detector using calculable parameters. Specular reflectance and internal quantum efficiency are separately estimated theoretically. Fresnel relations in three media with knowing of refractive indices of SiO_2 anti-reflection coating and Si substrate are given. The analytical model gives reasonable spectral responsivity results. Based on the comparison between the model and actual measurement, it has been observed that the analytical model is a simple solution for quantitative prediction of absolute spectral responsivity.

Keywords: responsivity, reflectance, quantum efficiency, trap detector, Fresnel relations.

1. INTRODUCTION

Knowledge of the spectral responsivity function is a fundamental requirement in various applications in radiometry, photometry, and colorimetry [1]. It can be described as the most important technical parameter for many types of photo-detectors, which can mirror the converting ability of the optical signal to electric current. Its measurement accuracy is quite critical for the development and research areas of the photo-detecting field [2]. The spectral responsivity of an ideal detector can be easily expressed in terms of fundamental constants, wavelength (λ) of the radiation and external quantum efficiency (EQE), (η_e) [3-7]. If a photodetector is an ideal i.e., η_e = 100 %, no losses will occur and the listed constants could describe entirely the ideal responsivity of such detector. This comes from the basic principle that each absorbed photon with energy greater than the semiconductor band gap produces exactly one charge carrier in the detector. The responsivity of a photodetector is thus given in units of Ampere/Watt [1, 8-10].

In reality, there is no perfect detector and the EQE is normally lower than 100%. The deviation from the ideal performance was caused by two loss mechanisms; reflectance from the surface of the diode and the non-ideal conversion of photons into measurable electron current or external and internal losses. Therefore, the responsivity of a real photodetector can be modeled as a modified ideal quantum detector [11].

At National Institute of Standards (NIS-Egypt), a transfer detector is used for calculating the spectral power responsivity in the wavelength range from 300 nm to 1000 nm. Figure-1 shows a 3-element reflection silicon photodiode trap detector, designed and fabricated in Hohenheide Inc. in Estonia. The detector was constructed with three Hamamatsu S1337 photodiodes, known for their high quality in radiometric applications [12].

Figure-1. NIS reflection trap detector.

In this work, the absolute spectral responsivity scale for the trap detector over the wavelength (300-1000) nm range can be modeled theoretically and described as a modified ideal quantum detector by a few parameters; the reflectance from the surface and others free parameters were taken into account. With knowing of refractive indices of SiO_2 anti-reflection coating and Si substrate, Fresnel equations in three media are used to estimate the reflectance from the photodiode surface. Our approach is to get a primary realization to estimate the absolute specular reflectance as well as the internal quantum efficiency (IQE), separately. A good estimation of these parameters allows precise extrapolation of the spectral responsivity of trap detectors and accurate suitable modeling of inter-reflections of trap detectors. The advantage of this approach is to get the possibility of pursuing interpolation of spectral responsivity without any loss of the physical meaning of the fitting parameters. Furthermore, there is no need for measuring light losses by reflection in the detector, which could be cumbersome for 3-element trap detectors.

2. THEORY

2.1 Spectral Responsivity Model

The responsivity of a real photodetector, $R(\lambda)$, can be modelled as a modified ideal quantum detector as [7, 13-15]:

$$R(\lambda)=\frac{e\lambda}{hc}(1-\rho(\lambda))\eta_i(\lambda)(1+g(\lambda)), \quad (1)$$

where $(e\lambda/hc)$ is the responsivity of an ideal quantum detector expressed by fundamental constants. (λ) is the wavelength of the applied radiation, $\rho(\lambda)$ is the spectrally dependent reflectance from the surface of a silicon photodiode and, $\eta_i(\lambda)$ is the IQE. In addition, $(1-\rho(\lambda))\ \eta_i(\lambda)$ is the EQE and directly can be realized using the experimental values of the absolute spectral power responsivity, as [10,16,17]:

$$\eta_e(\lambda)=1239.48\left(\frac{R(\lambda)}{\lambda}\right), \quad (2)$$

where λ is expressed in nm.

The quantum gain, g (λ), of a photodiode describes a rare situation, where the built-in voltage accelerates the charge carriers and secondary carriers are produced due to impact ionization. This contributed item is smaller than the loss corrections by the level of $g(\lambda) \approx 0.01$ ppm at temperatures below 100 K and decreases by two orders of magnitude at 300 K at the visible regime. Therefore, it will be neglected in our calculations and the reflectance in addition to the IQE using this model are separately estimated.

2.1.1 Reflectance model

Calculation of reflectance from a photodiode coated with a thin layer of silicon dioxide (SiO_2) on the silicon (Si) substrate requires methods used in thin film optics. The reflection and refraction of light at a surface between two media is governed by both the law of reflection and the Snell's law for the direction of the beam propagation, in addition to the Fresnel complex amplitude coefficients for the amplitude of the propagating waves [18]. Fresnel's equations is used to calculate the spectral reflectance over the whole spectrum with an uncertainty of less than of 1% from a single measurement, when the spectrally dependent refractive indices ($n_2(\lambda)$ for SiO_2 and $\bar{n}_3(\lambda)$ for Si) [13], polarization, angle of incidence and dioxide thickness are known. The values for $n_2(\lambda)$ and $\bar{n}_3(\lambda)$ used are taken from references [19,20].

The amplitude reflectance $r_{mn} = (\lambda,\theta)$ and the transmittance coefficients $t_{mn} = (\lambda,\theta)$ from medium m to n (m, n = 1, 2, 3) in the interface of two media can be calculated by using Fresnel equations [18].

For p-polarized beams, the coefficients are:

$$r_{mn}(\lambda,\theta)=\frac{n_n(\lambda)\cos(\theta_m)-n_m(\lambda)\cos(\theta_n)}{n_n(\lambda)\cos(\theta_m)+n_m(\lambda)\cos(\theta_n)}, \quad (3)$$

$$t_{mn}(\lambda,\theta)=\frac{2n_m(\lambda)\cos(\theta_m)}{n_n(\lambda)\cos(\theta_m)+n_m(\lambda)\cos(\theta_n)}, \quad (4)$$

and for s-polarized beams:

$$r_{mn}(\lambda,\theta)=\frac{n_m(\lambda)\cos(\theta_m)-n_n(\lambda)\cos(\theta_n)}{n_m(\lambda)\cos(\theta_m)+n_n(\lambda)\cos(\theta_n)}, \quad (5)$$

$$t_{mn}(\lambda,\theta)=\frac{2n_m(\lambda)\cos(\theta_m)}{n_m(\lambda)\cos(\theta_m)+n_n(\lambda)\cos(\theta_n)}, \quad (6)$$

Here, the reflectance and the transmittance coefficients are complex at the interface between Si and SiO_2 and depend upon the refractive indices, polarization, and angle of incidence. The phase difference between two subsequent wave fronts exiting the front surface of the SiO_2 layer is [13]:

$$\beta(\lambda,d)=\frac{2\pi}{\lambda}n_2(\lambda)d\ \cos(\theta_2(\lambda)), \quad (7)$$

where λ is the wavelength in air, d is the thickness of the dioxide layer and $\theta_2(\lambda)$ is the refractive angle in SiO_2 and can be calculated using the Snell's law. Evaluating the resulting geometrical series yields the amplitude reflection coefficient for the photodiode as [13]:

$$\bar{r}(\lambda,d)=r_{12}(\lambda)+\frac{t_{12}(\lambda)t_{21}(\lambda)\bar{r}_{23}(\lambda)\exp(-2i\,\beta(\lambda,d))}{1+r_{12}(\lambda)\bar{r}_{23}(\lambda)\exp(-2i\,\beta(\lambda,d))}. \quad (8)$$

The intensity reflection coefficient for s- and p-polarized beams can be calculated from the amplitude reflection coefficient as [13]:

$$\rho_{s,p}(\lambda,d)=|\bar{r}(\lambda,d)|^2. \quad (9)$$

By solving Eqs. (3-9) using the separating method, then the amplitude reflection coefficient for p-polarized beam, $\rho_p(\lambda, d)$, will be given as:

$$\rho_p(\lambda,d)=\left[r_{12}(\lambda)+A\frac{x_3x_4+y_3y_4}{x_4^2+y_4^2}\right]^2+\left[-A\frac{x_3y_4+x_4y_3}{x_4^2+y_4^2}\right]^2, \quad (10)$$

where $r_{12}(\lambda)=\frac{n_2(\lambda)\cos(\theta_1)-n_1(\lambda)\cos(\theta_2)}{n_2(\lambda)\cos(\theta_1)+n_1(\lambda)\cos(\theta_2)}$,

$A(\lambda)=t_{12}(\lambda)t_{21}(\lambda)$,

$t_{12}(\lambda)=\frac{2n_1(\lambda)\cos(\theta_1)}{n_2(\lambda)\cos(\theta_1)+n_1(\lambda)\cos(\theta_2)}$,

$t_{21}(\lambda)=\frac{2n_2(\lambda)\cos(\theta_2)}{n_1(\lambda)\cos(\theta_2)+n_2(\lambda)\cos(\theta_1)}$,

$x_4=\cos(2\beta(\lambda,d))+r_{12}(\lambda)x_3$,

$x_3=\frac{\left(n_3^2(\lambda)+k_3^2(\lambda)\right)\cos^2(\theta_2)-\left(x_2^2+y_2^2\right)n_2^2(\lambda)}{\left(n_3(\lambda)\cos(\theta_2)+n_2(\lambda)x_2\right)^2+\left(n_2(\lambda)y_2-k_3(\lambda)\cos(\theta_2)\right)^2}$,

$x_2=\frac{y_1^2+8x_1^2}{8x_1^{3/2}}$,

$x_1=1-\left(n_3^2(\lambda)-k_3^2(\lambda)\right)\left(\frac{n_1\sin(\theta_1)}{n_3^2(\lambda)+k_3^2(\lambda)}\right)^2$,

$y_4=\sin(2\beta(\lambda,d))+r_{12}(\lambda)y_3$,

$y_3=-\frac{2n_2(\lambda)\cos(\theta_2)\left(n_3(\lambda)y_2+x_2k_3(\lambda)\right)}{\left(n_3(\lambda)\cos(\theta_2)+n_2(\lambda)x_2\right)^2+\left(n_2(\lambda)y_2-k_3(\lambda)\cos(\theta_2)\right)^2}$,

$y_2=-\frac{y_1^2-8x_1^2y_1}{16x_1^{5/2}}$,

$y_1=-2n_3(\lambda)k_3(\lambda)\left(\frac{n_1(\lambda)\sin(\theta_1)}{n_3^2(\lambda)+k_3^2(\lambda)}\right)^2$,

and $(n_3(\lambda),k_3(\lambda))$ are the refractive index and extinction coefficient of Si, respectively. The amplitude reflection coefficient for s-polarized beam, $\rho_s(\lambda, d)$, will be given as:

$$\rho_s(\lambda,d)=\left[r_{12}(\lambda)+A\frac{M_3M_4+S_3S_4}{M_4^2+S_4^2}\right]^2+\left[-A\frac{M_3S_4+M_4S_3}{M_4^2+S_4^2}\right]^2, \quad (11)$$

where $r_{12}(\lambda)=\frac{n_1(\lambda)\cos(\theta_1)-n_2(\lambda)\cos(\theta_2)}{n_1(\lambda)\cos(\theta_1)+n_2(\lambda)\cos(\theta_2)}$,

$t_{12}(\lambda)=\frac{2n_1(\lambda)\cos(\theta_1)}{n_1(\lambda)\cos(\theta_1)+n_2(\lambda)\cos(\theta_2)}$,

$t_{21}(\lambda)=\frac{2n_2(\lambda)\cos(\theta_2)}{n_2(\lambda)\cos(\theta_2)+n_1(\lambda)\cos(\theta_1)}$,

$M_4=\cos(2\beta(\lambda,d))+r_{12}(\lambda)M_3$,

$M_3=\frac{n_2^2(\lambda)\cos^2(\theta_2)-\left(n_3^2(\lambda)+k_3^2(\lambda)\right)\left(x_2^2+y_2^2\right)}{\left(n_2(\lambda)\cos(\theta_2)+n_3(\lambda)x_2+k_3(\lambda)y_2\right)^2+\left(n_3(\lambda)y_2-k_3(\lambda)x_2\right)^2}$,

$S_4=\sin(2\beta(\lambda,d))+r_{12}(\lambda)S_3$,

$S_3=\frac{2n_2(\lambda)\cos(\theta_2)\left(k_3(\lambda)x_2+n_3(\lambda)y_2\right)}{\left(n_2(\lambda)\cos(\theta_2)+n_3(\lambda)x_2+k_3(\lambda)y_2\right)^2+\left(n_3(\lambda)y_2-k_3(\lambda)x_2\right)^2}$.

In a polarization-independent reflection trap detector, the incident beam is attenuated by five series reflections on the surface of the three photodiode surfaces before the residuals exit the device. Because of the triangular geometry of detector, the angle of incidence of these reflections is twice 45° for the s-polarized beam, once normal incidence, and twice 45° polarized beam. Thus the spectral specular reflectance of the trap detector is [13]:

$$\rho_{s,p}(\lambda,\theta_1,d)=\rho(\lambda,0^o,d)\rho_s^2(\lambda,45^o,d)\rho_p^2(\lambda,45^o,d). \quad (12)$$

2.1.2 Internal quantum efficiency model

Quantum efficiency is the ratio of countable photoelectrons produced to the number of photons incident on the photodiode. It is basically another way of expressing the effectiveness of the incident beam for producing electrical photo-current in a circuit [21,22]. The first attempts to establish a theoretical model for the IQE were made by the NIST-USA in 1980. The developed models of Geist et al. [23]and those improved by Gentile et al. [24]are two of the most widely used models. These models consider the probability for the incident photon to generate an electron-hole pair (e-h) that contributes to feeding photo-current to external circuitry. This probability depends upon only the depth of penetration of the photon in the silicon layer, i.e., it depends on its absorption coefficient.

The starting equation to calculate the IQE, $\eta_i(\lambda)$, of a silicon photodiode of thickness h is given by [25]:

$$\eta_i(\lambda)=\frac{\int_0^h P(x)\theta(\lambda)e^{-\alpha(\lambda)x}dx}{\int_0^h e^{-\alpha(\lambda)x}dx}, \quad (13)$$

where $P(x)$ is the collection efficiency at a depth x into the photodiode, $\theta(\lambda)$ is the quantum yield that is assumed to be unity for simplicity in the case of silicon over the desired wavelength range, and $\alpha(\lambda)$ is the absorption coefficient of silicon at wavelength λ and given by the imaginary part extinction coefficient:

$$\alpha(\lambda)=\frac{4\pi}{\lambda}k_3(\lambda). \quad (14)$$

Then, Eq. (13) can be rewritten as [4,24-28]:

$$\eta_i(\lambda) = \int_0^h e^{-\alpha(\lambda)x}\,\alpha(\lambda)P(x)dx\,. \quad (15)$$

By solving Eq. (15) for $P(x)$, it yields [6, 13, 26, 28, 29]:

$$\eta_i(\lambda) = P_f + \frac{1-P_f}{\alpha(\lambda)T}\{1-e^{-\alpha(\lambda)T}\} - \frac{1-P_r}{\alpha(\lambda)[D-T]}\{e^{-\alpha(\lambda)T} - e^{-\alpha(\lambda)D}\} - P_r e^{-\alpha(\lambda)h}, \quad (16)$$

where the parameters P_f and P_r are the collection efficiencies in the front and rear regions, respectively. T and D are the depths at which the space-charge region begins and finishes, respectively. For simplicity, only the portion of the spectral region from 400 to 900 nm is taking into account. In this case, the parameter D was eliminated and hence the collection efficiency simply rises from a value of P_f at the front of the diode to a value P_r over a distance T, and stays fixed at P_r to the back of the diode. Therefore, the last term in Eq. (16) can be omitted and rewritten as [29, 30]:

$$\eta_i(\lambda) = P_f + \frac{P_r - P_f}{\alpha(\lambda)T}\{1-e^{-\alpha(\lambda)T}\}, \quad (17)$$

where the parameters P_f, P_r, and T are used as fitting parameters that should be adjusted in such a way that the model data have the best fit to the experimental data.

The consistency between the calculated results and the corresponding experimental data is tested by estimating χ^2 as follows [31]:

$$\chi^2 = \sum_{\lambda_{min.}}^{\lambda_{max.}} \frac{\left(R_{exp.}(\lambda) - R_{calc.}(\lambda)\right)^2}{R^2_{exp.}(\lambda)}, \quad (18)$$

where $R_{exp.}(\lambda)$ is the experimental data of the absolute spectral responsivity and $R_{calc.}(\lambda)$ is the calculated values of the responsivity model.

3. MODELING RESULTS

3.1 Spectral Reflectance

The thickness of the SiO_2 layer in Hamamatsu S1337 silicon photodiode was assumed to be 30.0 nm in the calculation of spectral reflectance [6, 29, 30, 32, 33]. This approximated value gives a reasonable agreement with both the attained experimental values and the theoretical prediction of the spectral responsivity. This indicates that the derived Eqs. (10) and (11) using Fresnel relations with an oxide thickness of 30.0 nm is a good model for this type of Si photodiodes that matches with almost all measurement geometries. The model results together with the corresponding reflectance values calculated in section 2.1.1 are presented in Figure-1 and Figure-2 for s- and p-polarized beams with respect to normal incidence, respectively. Figure-4 shows the resulting spectral reflectance of trap detector, considering the 3-element S1337 photodiode construction in the wavelength range from 300 nm to 1000 nm.

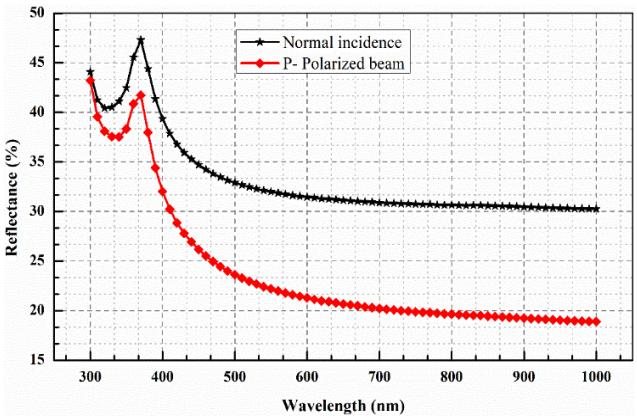

Figure-1. Calculated spectral reflectance of S1337 photodiode for p-polarized beam at 45° angle of incidence compared to normal incidence at the wavelength range (300 - 1000) nm.

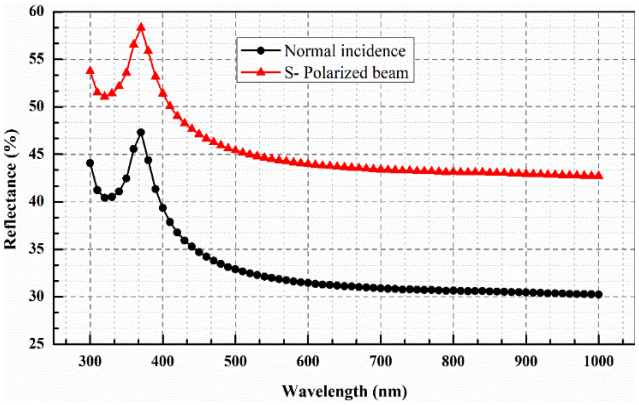

Figure-2. Calculated spectral reflectance of S1337 photodiode for s-polarized beam at 45° angle of incidence compared to normal incidence at the wavelength range (300 - 1000) nm.

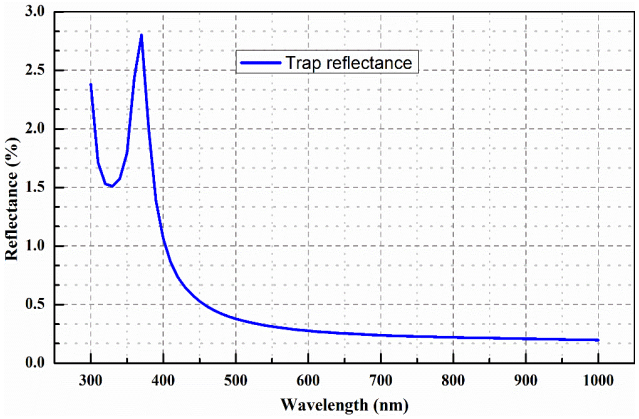

Figure-3. Calculated spectral reflectance of trap detector with thin-film Fresnel relations at 30.0 nm SiO_2 layer thickness.

3.2 Quantum Efficiency and Responsivity Scale

Direct fitting of the EQE was accomplished by constructing a numerical model depending on the spectral reflectance approach of the trap detector, see Eq. (12) and the given physical model for the IQE, see Eq. (17). This model was used to fit values of the EQE determined at wavelength range 300 nm to 1000 nm as shown in Figure-4. The fitting parameters are: P_f= 0.977, P_r = 0.9997, T = 390 µm and d = 30.0 nm. They can be understood on the basics of the model of Geist *et al* [23]. as if all incident beams are absorbed up to the end of the depletion region. This is valid because the model is limited to the visible regime. Therefore, the collection efficiency increases from the Si/SiO_2 interface value (0.977) up to (0.9997) at a depth of 390 µm, from where begins the depletion region. Therefore, the calculated results of the EQE are in a good agreement with those obtained experimentally over the wavelength range only from 400 nm to 900 nm as shown in Figure-5.

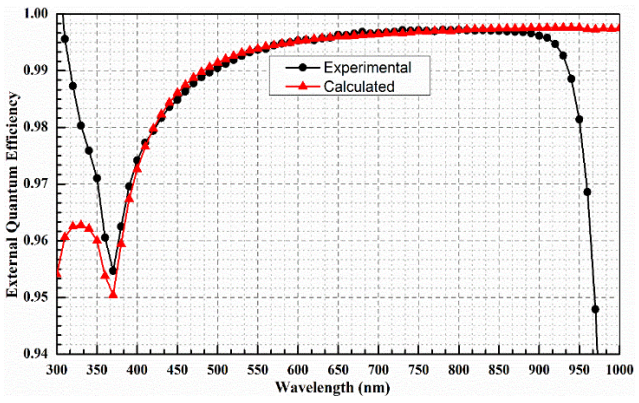

Figure-4. Calculated and experimental values of EQE for trap detector in the 300 nm to 1000 nm wavelength range.

Figure-6 shows the measured results of the absolute spectral responsivity of the trap detector with a black solid line between 300 nm to 1000 nm wavelength range. These results are presented and compared with the model values obtained by the best parameter of optimization P_f, P_r, T and d as illustrated with a dotted red line. These measurements were performed at the national metrology institute of Finland, MIKES, over the wavelength range (300 - 1000) nm with an increment of 10 nm. The relative expanded uncertainty ranges from 0.5 % to 4.0 %, depending on the calibrated wavelength regime. The χ^2 value of the calculated and the measured data in the range (400 - 900) nm was estimated to be 2.85×10^{-5} approximately. This value gives a reasonable agreement with the measured results at the desired wavelength range. In the wavelength range (300 - 1000) nm, theχ^2 value equals 9.67×10^{-2}. One noticed that this value is very huge compared to the previous ones due to two reasons. Firstly, the silicon absorption in the near infrared region is further reduced and photons penetrate behind the depletion region. Hence, the probability of pair recombination before collection is high and so that the quantum efficiency is reduced. Secondly, the used simplified IQE model is considered only the range of visible spectral regime, see Eq. (17). Therefore, the last term in Eq. (16) was omitted and the parameter D was eliminated. As a result, the calculated and measured results are matched over most of spectral range. Hence, these results are successfully in a good agreement for the physical fitting parameters of the IQE and the mathematical model of the spectral reflectance for trap detector.

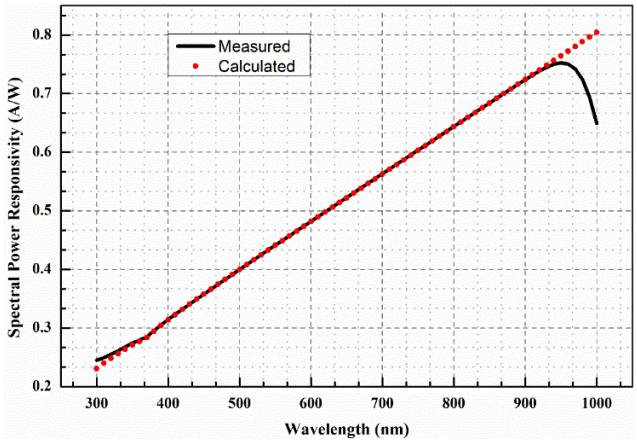

Figure-5. Calculated and measured absolute spectral power responsivity of the trap detector over the wavelength range from 300 nm to 1000 nm.

4. CONCLUSIONS

The absolute spectral responsivity of a 3-element silicon trap detector is predicted and gave successfully a reasonable agreement for the experimental data within the wavelength range (300 <λ (nm) <1000) using the fitting parameters P_f, P_r, T and d. A new mathematical equation for calculating the absolute spectral reflectance with a three photodiode model S1337 was derived in this work and showed a good fitting with measured values besides the modeled IQE. The main advantage of this approach is the ability to pursue interpolation of spectral responsivity without any loss of physical meaning of the fitted

parameters. Furthermore, there is no need for measurement of light losses by reflection in the detector, which could be cumbersome for 3-element trap detectors.

REFERENCES

[1] M. Ghazeer, A. Abdelmageed, A. Hassen. 2018. Realization of spectral irradiance responsivity at NIS-Egypt, Optik. 168, 390-395. doi:10.1016/j.ijleo.2018.04.094.

[2] H. Meng, L. Xiong, N. Xu, Y. He, J. Zhang, B. Zhang. 2018. Calibration of photo-detector's absolute spectral responsivity in the wavelength range 300 nm to 1000 nm, Int. Conf. Opt. Instruments Technol. Optoelectron. Meas. Technol. Syst., Proc. SPIE: p. 82. doi:10.1117/12.2295479.

[3] S. Chen, C. Teng, M. Zhang, Y. Li, D. Xie, G. Shi. 2016. A Flexible UV-Vis-NIR photodetector based on a Perovskite/Conjugated-Polymer composite, Adv. Mater. 28, 5969-5974. doi:10.1002/adma.201600468.

[4] A. L. Muñoz Zurita, J. Campos Acosta, R. Gómez Jiménez, J. Rojas Domenico, A. S. Shcherbakov. 2010. Study of some optoelectronics characteristics of InGaAs/InP photodetectors, Proc. SPIE: p. 772629. doi:10.1117/12.854900.

[5] S. Mukherjee, R. Maiti, A. K. Katiyar, S. Das, S. K. Ray. 2016. Novel colloidal MoS2 quantum dot heterojunctions on silicon platforms for multifunctional optoelectronic devices, Sci. Rep. 6, 29016. doi:10.1038/srep29016.

[6] K.-S. Hong, S. Park, S.-K. Kim, S.-N. Park, D.-H. Lee. 2015. Realization of the spectral responsivity scale based on an absolute cryogenic radiometer, J. Korean Phys. Soc. 67, 2045-2058. doi:10.3938/jkps.67.2045.

[7] T. Menegotto, T. F. Da Silva, M. Simões, W. A. T. De Sousa, G. Borghi. 2015. Realization of optical power scale based on cryogenic radiometry and trap detectors, IEEE Trans. Instrum. Meas. 64, 1702-1708. doi:10.1109/TIM.2014.2383072.

[8] S. M. Reda, A. A. Abdelmageed, A. S. Monem, R. H. El-Gebaly, S. M. Faramawy. 2018. Estimation of spectral mismatch correction factor f1 indicated by radiometer responsivity toward phototherapic infant devices, Appl. Opt. 57, 9615-9619. doi:https://doi.org/10.1364/AO.57.009615 1.

[9] K. Hong, P. Seongchong, J. Hwang, E. Atkinson, P. Manson, D.-H. Lee. 2017. Spectral responsivity measurement of photovoltaic detectors by comparison with a pyroelectric detector on individual nano-second laser pulses, Metrologia. 54, 355-364.doi: 10.1088/1681-7575/aa5b65.

[10] I. Müller, U. Johannsen, U. Linke, L. Socaciu-Siebert, M. Smîd, G. Porrovecchio, M. Sildoja, F. Manoocheri, E. Ikonen, J. Gran, T. Kübarsepp, G. Brida, L. Werner. 2013. Predictable quantum efficient detector: II. Characterization and confirmed responsivity, Metrologia. 50, 395-401. doi:10.1088/0026-1394/50/4/395.

[11] T. Dönsberg, F. Manoocheri, M. Sildoja, M. Juntunen, H. Savin, E. Tuovinen, H. Ronkainen, M. Prunnila, M. Merimaa, C. K. Tang, J. Gran, I. Müller, L. Werner, B. Rougié, A. Pons, M. Smîd, P. Gál, L. Lolli, G. Brida, M. L. Rastello, E. Ikonen. 2017. Predictable quantum efficient detector based on n-type silicon photodiodes, Metrologia. 54, 821-836. doi:10.1088/1681-7575/aa85ed.

[12] R. Goebel, M. Stock. 1998. Nonlinearity and polarization effects in silicon trap detectors, Metrologia. 35, 413-418. doi:10.1088/0026-1394/35/4/33.

[13] J. Gran, A. S. Sudbø. 2004. Absolute calibration of silicon photodiodes by purely relative measurements, Metrologia. 41, 204-212. doi:10.1088/0026-1394/41/3/014.

[14] J. C. Zwinkels, E. Ikonen, N. P. Fox, G. Ulm, M. L. Rastello. 2010. Photometry, radiometry and "the candela": evolution in the classical and quantum world, Metrologia. 47, R15-R32. doi: 10.1088/0026-1394/47/5/R01

[15] J. Gran, T. Kübarsepp, M. Sildoja, F. Manoocheri, E. Ikonen, I. Müller. 2012. Simulations of a predictable quantum efficient detector with PC1D, Metrologia. 49, S130-S134. doi:10.1088/0026-1394/49/2/S130.

[16] A. L. Muñoz Zurita, J. Campos Acosta, R. Gomez Jimenez, R. Uribe Valladares. 2010. An absolute radiometer based on InP photodiodes, Proc. SPIE: p. 772628. doi:10.1117/12.854898.

[17] G. Eppeldauer, M. Rácz. 2000. Spectral power and irradiance responsivity calibration of InSb working-

standard radiometers, Appl. Opt. 39, 5739. doi:10.1364/AO.39.005739.

[18] A. Haapalinna, P. Kärhä, E. Ikonen. 1998. Spectral reflectance of silicon photodiodes, Appl. Opt. 37, 729. doi:10.1364/AO.37.000729.

[19] I. H. Malitson. 1965. Interspecimen comparison of the refractive index of fused silica*†, J. Opt. Soc. Am. 55, 1205. doi:10.1364/JOSA.55.001205.

[20] G. E. Jellison, 1992. Optical functions of silicon determined by two-channel polarization modulation ellipsometry, Opt. Mater. 1, 41-47. doi: 10.1016/0925-3467(92)90022-F.

[21] Ö¨ Bazkir, F. Samadov. 2005. Characterization of silicon photodiode-based trap detectors and establishment of spectral responsivity scale, Opt. Lasers Eng. 43, 131-141. doi:10.1016/j.optlaseng.2004.08.004.

[22] R. K. Ulaganathan, Y.-Y. Lu, C.-J. Kuo, S. R. Tamalampudi, R. Sankar, K. M. Boopathi, A. Anand, K. Yadav, R. J. Mathew, C.-R. Liu, F.C. Chou, Y.-T. Chen. 2016. High photosensitivity and broad spectral response of multi-layered germanium sulfide transistors, Nanoscale. 8, 2284-2292. doi:10.1039/C5NR05988G.

[23] E. F. Zalewski, J. Geist. 1980. Silicon photodiode absolute spectral response self-calibration, Appl. Opt. 19, 1214-1216. doi: 10.1364/AO.19.001214

[24] T. R. Gentile, J. M. Houston, C. L. Cromer. 1996. Realization of a scale of absolute spectral response using the National Institute of Standards and Technology high-accuracy cryogenic radiometer, Appl. Opt. 35, 4392. doi:10.1364/AO.35.004392.

[25] A. Ferrero, J. Campos, A. Pons, A. Corrons. 2005. New model for the internal quantum efficiency of photodiodes based on photocurrent analysis, Appl. Opt. 44, 208-216. doi:10.1364/AO.44.000208.

[26] L. Werner, J. Hartmann. 2009. Calibration and interpolation of the spectral responsivity of silicon photodiode-based detectors, Sensors Actuators a Phys. 156, 185-190. doi:10.1016/j.sna.2009.05.002.

[27] J. Geist. 1979. Quantum efficiency of the p-n junction in silicon as an absolute radiometric standard, Appl. Opt. 18, 1978-1980. doi:10.1364/AO.18.000760.

[28] C. Hicks, M. Kalatsky, R. A. Metzler, A. O. Goushcha, Quantum efficiency of silicon photodiodes in the near-infrared spectral range, Appl. Opt. 42 (2003) 4415-4422. doi:10.1364/AO.42.004415.

[29] T. Kübarsepp, P. Kärhä, E. Ikonen. 2000. Interpolation of the spectral responsivity of silicon photodetectors in the near ultraviolet, Appl. Opt. 39, 9-15. doi:10.1364/AO.39.000009.

[30] T. R. Gentile, S. W. Brown, K. R. Lykke, P. S. Shaw, J. T. Woodward. 2010. Internal quantum efficiency modeling of silicon photodiodes, Appl. Opt. 49, 1859-1864. doi:10.1364/AO.49.001859.

[31] C. Xiangzhou, F. Jun, S. Wenqing, W. Jiansong, Y. Wei. 1998. In-medium nucleon-nucleon cross section and its effect on total nuclear reaction cross section, Phys. Rev. c. 58, 572-575. doi:https://doi.org/10.1103/PhysRevC.58.572.

[32] L.-P. Boivin. 2001. Spectral responsivity of various types of silicon photodiode at oblique incidence: comparison of measured and calculated values, Appl. Opt. 40, 485. doi:10.1364/AO.40.000485.

[33] T. Menegotto, M. S. Lima, G. B. Almeida, I. B. Couceiro, H. P. Grieneisen. 2011. Direct modeling of external quantum efficiency of silicon trap detectors, Proc. SPIE, p. 808313. doi:10.1117/12.889436.